Frictional Melting in Hydrothermal Fluid-Rich Faults: Field and Experimental Evidence From the Bolfín Fault Zone (Chile)

R. Gomila, M. Fondriest, E. Jensen, E. Spagnuolo, S. Masoch, T. M. Mitchell, G. Magnarini, A. Bistacchi, S. Mittempergher, D. Faulkner, et al.

Key Points:
- The Bolfin Fault Zone shows the first pseudotachylytes described in the Atacama Fault System giving insights of past seismic activity
- Rotary shear experiments at seismic slip velocities resulted in formation of vesiculated pseudotachylytes in all tested conditions
- Natural pseudotachylytes formed in a hydrothermal fluid-rich environment where vesiculation is related to CO_2 degassing from calcite veins

Frictional Melting in Hydrothermal Fluid-Rich Faults: Field and Experimental Evidence From the Bolfín Fault Zone (Chile)

R. Gomila[1] , M. Fondriest[1,2] , E. Jensen[3] , E. Spagnuolo[4] , S. Masoch[1] , T. M. Mitchell[5] , G. Magnarini[5] , A. Bistacchi[6] , S. Mittempergher[7] , D. Faulkner[8] , J. Cembrano[9] , and G. Di Toro[1,4]

[1]Dipartimento di Geoscienze, Università degli Studi di Padova, Padova, Italy, [2]Institut des Sciences de la Terre (ISTerre), Université Grenoble Alpes, Grenoble, France, [3]Departamento Ingeniería y Ciencias Geológicas, Universidad Católica del Norte, Antofagasta, Chile, [4]Istituto Nazionale di Geofisica e Vulcanologia, Rome, Italy, [5]UCL Earth Sciences, University College of London, London, UK, [6]Dipartimento di Scienze dell'Ambiente e della Terra, Università di Milano-Bicocca, Milano, Italy, [7]Dipartimento di Scienze Chimiche e Geologiche, Università di Modena e Reggio Emilia, Modena, Italy, [8]School of Environmental Sciences, University of Liverpool, Liverpool, UK, [9]Escuela de Ingeniería, Pontificia Universidad Católica de Chile, Santiago de Chile, Chile

Abstract Tectonic pseudotachylytes are thought to be unique to certain water-deficient seismogenic environments and their presence is considered to be rare in the geological record. Here, we present field and experimental evidence that frictional melting can occur in hydrothermal fluid-rich faults hosted in the continental crust. Pseudotachylytes were found in the >40 km-long Bolfín Fault Zone of the Atacama Fault System, within two ca. 1 m-thick (ultra)cataclastic strands hosted in a damage-zone made of chlorite-epidote-rich hydrothermally altered tonalite. This alteration state indicates that hydrothermal fluids were active during the fault development. Pseudotachylytes, characterized by presenting amygdales, cut and are cut by chlorite-, epidote- and calcite-bearing veins. In turn, crosscutting relationship with the hydrothermal veins indicates pseudotachylytes were formed during this period of fluid activity. Rotary shear experiments conducted on bare surfaces of hydrothermally altered rocks at seismic slip velocities (3 m s^{-1}) resulted in the production of vesiculated pseudotachylytes both at dry and water-pressurized conditions, with melt lubrication as the primary mechanism for fault dynamic weakening. The presented evidence challenges the common hypothesis that pseudotachylytes are limited to fluid-deficient environments, and gives insights into the ancient seismic activity of the system. Both field observations and experimental evidence, indicate that pseudotachylytes may easily be produced in hydrothermal environments, and could be a common co-seismic fault product. Consequently, melt lubrication could be considered one of the most efficient seismic dynamic weakening mechanisms in crystalline basement rocks of the continental crust.

1. Introduction

Tectonic pseudotachylytes are solidified frictional melts, formed within faults during co-seismic slip (Maddock, 1983; Sibson, 1975), and are considered to be unambiguous evidence of past earthquakes (Cowan, 1999; Rowe & Griffith, 2015). Despite the clear seismic origin of pseudotachylytes, there has been a long debate regarding the environmental conditions during their formation within fault zones. While some authors argued in favor of a water-deficient environment condition hypothesis for pseudotachylyte formation (Sibson, 1975; Sibson & Toy, 2006), there is a growing body of research pointing toward pseudotachylyte formation in "wet" environments (Allen, 1979; Bjørnerud, 2010; Boullier et al., 2001; Famin et al., 2008; Magloughlin, 2011; Rowe et al., 2005; Williams et al., 2017). We define a wet environment as a rock volume with fluids available in the form of (a) free pore water (i.e., hydrothermal fluids), or (b) volatile-rich minerals (e.g., hydrous minerals). Pirajno (2009) defined a hydrothermal fluid as a hot (∼50 to >500°C) aqueous solution (with H_2O as solvent), containing solutes (including CO_2, CH_4 and diverse anions and cations) that are commonly precipitated as the solution changes its properties in space and time.

According to several authors (e.g., Bjørnerud, 2010; Maddock, 1992; Magloughlin, 1989, 1992; Meneghini et al., 2010), the formation of pseudotachylytes could be enhanced by the presence of cataclasites. Indeed,

this fine-grained and often water-rich fault material (e.g., presence of hydrous minerals as epidote, chlorite, etc., free water within pores and fluid inclusions), would lower the melting point of the fault rock assemblage and promote frictional melting during seismic slip (Lee et al., 2017; Magloughlin & Spray, 1992; Spray, 1992). Hence, fault rocks enriched in hydrous minerals would favor pseudotachylyte formation. However, during seismic slip, pore water may absorb heat and expand, and trigger fault weakening by thermal pressurization if the fluids are trapped within the fault slipping zone (Lachenbruch, 1980; Sibson, 1973). Thermal pressurization, if efficient, would buffer the temperature increase in the slipping zone and prevent frictional melting (Rice, 2006).

Vesicles in pseudotachylytes have been first described in the early work of Nockolds (1940) and Philpotts (1964) who pointed out the idea that the abundance of amygdales (mineral-filled vesicles) in pseudotachylytes suggests that the liquids from which these rocks were formed must have been highly charged with gases, giving the first hints that some sort of fluid or vapor phase must be present at the time of pseudotachylyte generation. Whilst Maddock et al. (1987, 1989), argued for the use of vesicle abundance in pseudotachylytes as a proxy for palaeoseismic depth, Dixon and Dixon (1987) suggested that a small amount of free water in the fault zone could be responsible for their formation. Later work performed on subduction complexes (e.g. Meneghini et al., 2010; Phillips et al., 2019; Rowe et al., 2005; Ujiie, Yamaguchi, et al., 2007) showed that the presence of vesicles in pseudotachylytes formed in this fluid-rich environment is also possible.

Previous experimental evidence suggests that friction melting in silicate rocks is possible under water-saturated conditions (Violay, Di Toro, et al., 2015; Violay, Nielsen, et al., 2014). The experiments showed that both microgabbro and basalt melt under effective normal stress (σ_n^{eff}) of 20 MPa and pore fluid pressure (P_f) of 5 MPa, resulting in a slipping zone with glassy matrix full of vesicles, although no further attention was given to this texture in these studies.

In this paper we describe the first pseudotachylytes recognized in the Atacama Fault System (AFS) in Northern Chile, characterized by the presence of amygdales both, spatially and temporally associated with foliated hydrothermally altered fault-core rocks in a strong fluid-rock interaction environment. We then investigate the conditions controlling the formation of vesicles in frictional melts originated from volatile-enriched cataclasites, through a series of high velocity friction experiments at different fluid pore pressures on the same cataclasites hosting the natural pseudotachylytes, with the aim to understand at which conditions vesiculated pseudotachylytes can be produced. Vesicles were produced at all tested conditions, but we demonstrate that while they can be generated by mineral dehydration (chlorite, etc.) in experimental samples, in nature they are most likely derived from CO_2 (derived from calcite in the fault rock assemblage) exsolved from the melt.

2. Geological Setting

The main structural feature of the Coastal Cordillera, in northern Chile, corresponds to the N–S trending, trench-parallel, Atacama Fault System (AFS; Arabasz, 1971; Scheuber & González, 1999). The AFS is ca. 1,000 km-long and records left-lateral finite shear, interpreted as a response of the oblique subduction of the Aluk (Phoenix) plate beneath the South American plate during the Mesozoic (Figure 1).

Deformation along the AFS is both spatially and temporally related to the magmatism of the Coastal Cordillera, with pluton cooling and crystallization ages between 150 and 110 Ma (Olivares et al., 2010; Ruthven et al., 2020; Scheuber et al., 1995; Seymour et al., 2020). The central segment of the AFS is ca. 150 km-long and it consists of (a) steeply dipping sinistral strike-slip duplexes with a hierarchical pattern of master and subsidiary faults, fault-veins and veins (i.e., mode I + II/III and mode I filled fractures, respectively), developed in a transtensional regime near Antofagasta, at 24°S (Figure 1a) (Cembrano et al., 2005; Jensen et al., 2011; Olivares et al., 2010; Veloso et al., 2015) and (b) steeply dipping sinistral mylonitic fabrics overprinted by brittle faults developed in a transpressional regime at ca. 25°S (Ruthven et al., 2020). The hydrothermal nature of fluid transport in the northern part of the central segment has been largely documented by several authors (Arancibia et al., 2014; Gomila et al., 2016; Herrera et al., 2005; Veloso et al., 2015) as a pervasive fault-related chloritic and propylitic alteration evidenced by a widespread chlorite-epidote-calcite
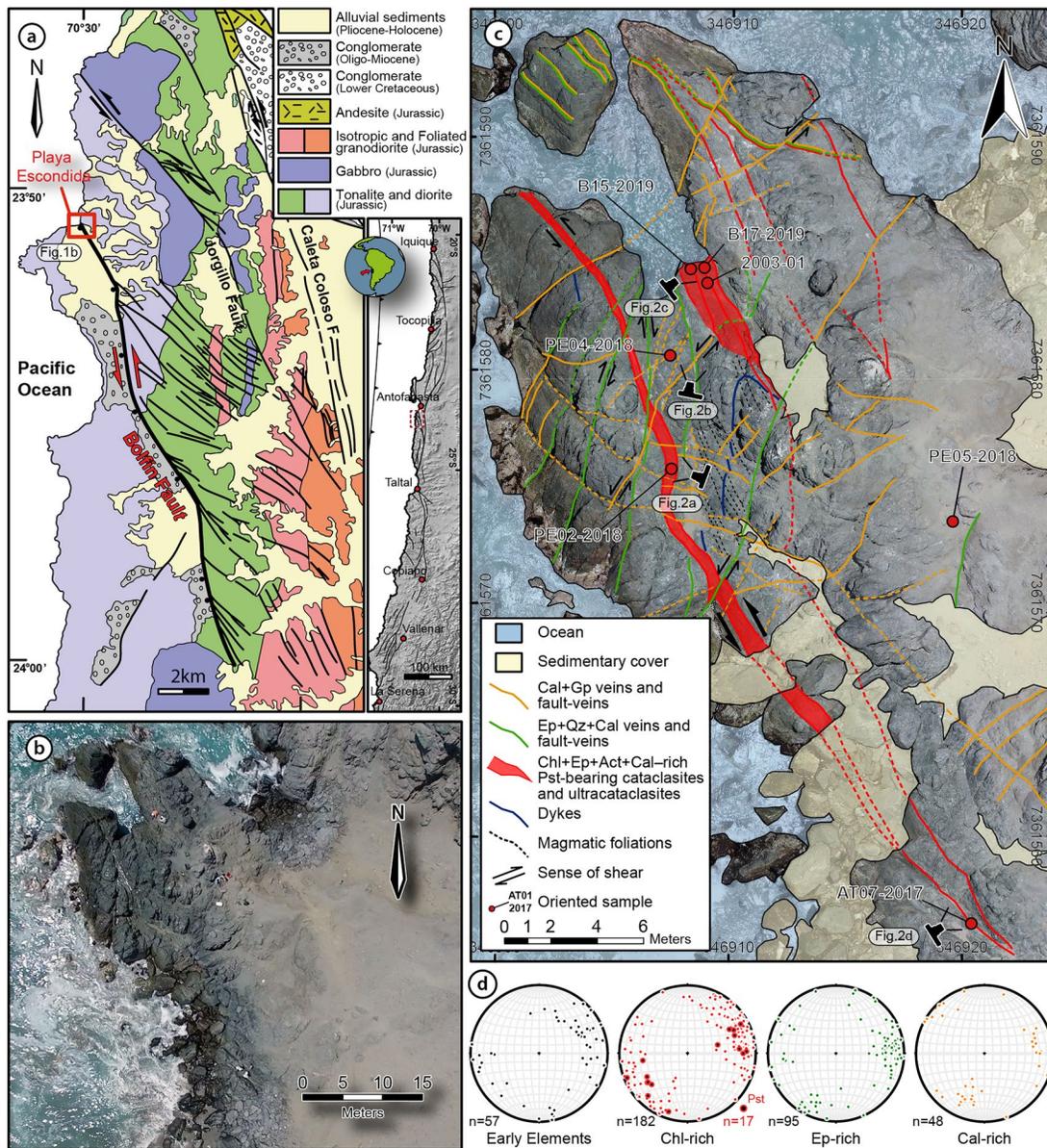
Figure 1. The Playa Escondida Outcrop. (a) Geological setting and simplified structural map of the northern part of the Bolfin Fault Zone, located in the Atacama Fault System, in the western border of northern Chile (modified from Cembrano et al. [2005]). (b) Aerophotograph of the Playa Escondida Outcrop of the Bolfin Fault Zone. Note the green-colored western side of the outcrop due to pervasive chlorite precipitation. (c) Structural map showing the presence of two main sub-parallel fault-cores ca. 1 m-thick and the cross-cutting relations of the fault and fracture network. (d) Structural data of the different stages according to their timing and main mineral phase. Poles to planes (n: number of planes) of the different structural elements (magmatic foliations, faults, fault-veins and veins). Early Elements consist of early formed structural elements (i.e., before brittle faulting occurred) such as magmatic foliations and basaltic to andesitic dykes; chlorite-rich stage consists of faults and fault-veins temporally and spatially associated with chlorite infills, chlorite-epidote-rich foliated cataclasites with minor amounts of calcite, chlorite-epidote-calcite veins and pseudotachylyte fault-veins. The epidote-rich stage is represented by faults and fault-veins marked by hydrothermal epidote, quartz and minor calcite precipitation, whereas the calcite-rich stage consists of faults filled with calcite (±gypsum ± palygorskite ± halite); Pst: pseudotachylyte, Chl: chlorite, Ep: epidote, Cal: calcite, Gp: gypsum, Qz: quartz, Act: actinolite.

precipitation. Studies on chlorite geothermometry of Arancibia et al. (2014) established an average $T_{chlorite}$ values of 323°C based on the tetrahedral Al occupancy in chlorite, obtained from the Caleta Coloso Fault (Figure 1a), implying that the maximum depth constrain of hydrothermal alteration and faulting is around 6–8 km, assuming a geothermal gradient between 40 and 50°C/km.

The Bolfín Fault Zone, located in the northern part of the central segment of the AFS, is a NNW- to NW-trending left-lateral strike-slip fault zone, which is exposed over a minimum length of ca. 45 km (since it runs beneath the ocean in its northern sector; Figure 1). The fault zone is exposed almost continuously from the northern border of the Playa Escondida sector (Figures 1b and 1c) until it merges with the Caleta Coloso Fault Zone at an angle of 20° (González, 1999; González & Niemeyer, 2005). The Bolfín Fault Zone cuts through Late Jurassic – Early Cretaceous crystalline rocks belonging to the meta-diorites and meta-gabbros of the Bolfín Complex and the tonalitic to granodioritic unit of the Cerro Cristales Pluton (Figure 1a).

3. Methods

We integrated Unmanned Aerial Vehicle (UAV) photo surveys with detailed field mapping of ductile shear zones, brittle faults and fault-veins of the Bolfín Fault Zone at the Playa Escondida outcrop to produce a high-resolution structural map (Figure 1c). We used a DJI Phantom 4 Pro drone, from which 48 nadir-directed aerophotographs were taken at a mean flight elevation of 10 m over the ground level. The images were processed in Agisoft Photoscan Pro to generate a high-resolution georeferenced orthomosaic image with a spatial resolution of ca. 0.6 cm/pix (Figure 1c).

Twenty oriented fault rock samples were collected from the Playa Escondida outcrop. Most were used for microstructural, geochemical and mineralogical investigations, while two large block samples were used for rotary shear experiments (samples B21 and B23). The blocks were big enough to drill 50 mm in diameter and ca. 60 mm-long cores to be used in rotary-shear experiments (see Figure S1).

The experiments were performed with the Slow to HIgh Velocity Apparatus (SHIVA) installed at the High Pressure-High Temperature (HPHT) Laboratory of the Istituto Nazionale di Geofisica e Vulcanologia (INGV) in Rome (for details about the experimental machine, its calibration, acquisition and sample preparation, see Di Toro, Niemeijer, et al., 2010; Nielsen et al., 2008; Niemeijer et al., 2011). We performed six experiments under different environmental conditions: two at room humidity, two in the presence of pressurized distilled water ($P_f = 5$ MPa), one under vacuum (10^{-4} mbar) and one using steam on dry surfaces. The rock specimens were slid following a trapezoidal velocity function with target slip rates (velocity, V) of 3 m s^{-1}, acceleration of 25 m s^{-2} and total slip (displacement) of 1 m under an effective normal stress (σ_n^{eff}) of 20 MPa (see Table S1). Exceptions to these general conditions are experiments s1688 (which had 6.3 m s^{-2}), s1691 (3 m of slip) and s1690 (with an σ_n^{eff} of 15 MPa).

The mineral chemistry of the pseudotachylyte matrix and of the rock-forming minerals (plagioclase, amphibole, epidote, chlorite, etc.) were obtained by several methods. First, wavelength-dispersive electron microprobe analyses (EMPA), were carried out on polished thin sections at INGV, Rome, with Joel-JXA8200 microprobe equipped with EDS-WDS. Analytical conditions were 15 kV as accelerating voltage, a beam current of 7.5 nA and a spot size of 3 µm. Second, semi-quantitative X-ray powder diffraction (XRPD) analyses were carried out at UNIPD, Padova, through the Reference Intensity Ratio method with a PANalytical X'Pert Pro diffractometer equipped with a Co radiation source, operating at 40 mA and 40 kV in the angular range 3° < 2θ < 85°. Lastly, a Zeiss FEG Gemini 500 Field Emission Scanning Electron Microscope (FE-SEM), equipped with a Brucker QUANTAX EBSD, was used to analyze mineral chemistry of the experimentally produced pseudotachylyte matrix at the University of Milano-Bicocca, Italy. Analytical conditions were 20 kV as accelerating voltage and a spot size of 0.7 µm.

4. The Playa Escondida Outcrop

The Playa Escondida outcrop covers an area of ca. 20×40 m^2 and is located where the Bolfín Fault Zone enters in the Pacific Ocean, at the northern end of the fault (Figure 1b). At the outcrop (Figure 1c), the Bolfín Fault Zone corresponds of a N30W-striking and SW-subvertical dipping fault-core composed of two strands of ca. 1 m-wide foliated cataclasites. The damage zone consists of poorly to intensively altered tonalites showing magmatic foliations and up to a few centimeters thick layers of cataclasites along subsidiary faults (Figure 2).
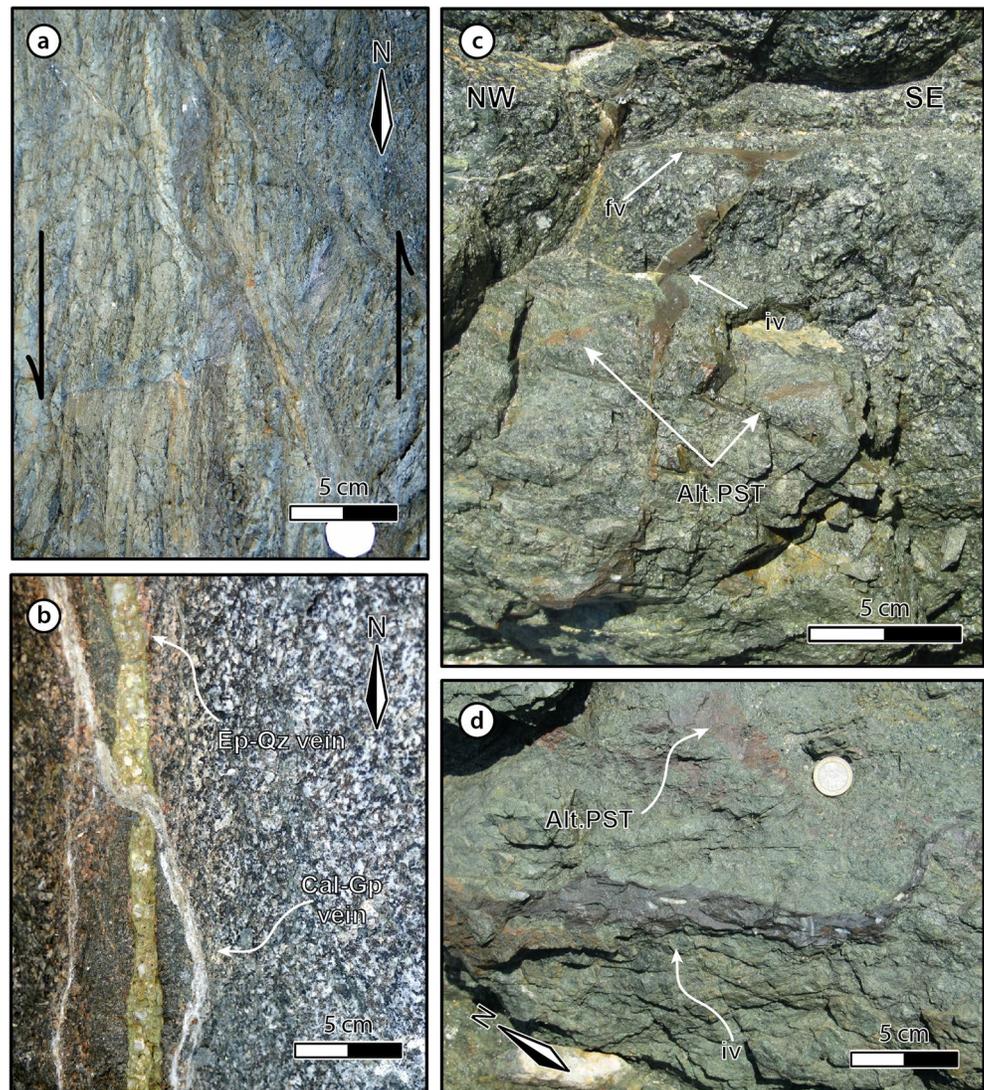
Figure 2. Fault zone rock assemblage of the Playa Escondida Outcrop. (a) Foliated chlorite-epidote-rich foliated cataclasites in hydrothermally altered fault-core. (b) Multiple veins cutting the hydrothermally altered fault rocks hosted in tonalite to quartz-diorite, suggesting several episodes of fluid infiltration. Note epidote-quartz vein cut by calcite-gypsum vein. (c and d) Multiple generations of pseudotachylytes cutting altered cataclasites and poorly to intensively altered tonalites to quartz-diorites. Note dismembered red-altered pseudotachylytes within the chlorite-rich fault-core. Alt. PST: altered pseudotachylytes; iv: injection vein; fv: fault-vein; Qz: quartz; Ep: epidote; Cal: calcite; Gp: gypsum. For location of the photos refer to Figure 1c.

Based on the structural features and mineral assemblage, and on their crosscutting relationships observed in the field (Figure 2), four main deformation stages were recognized (Figure 1d): (a) an "early" stage, consisting of NW- to N-striking early structural elements consisting of magmatic foliations and non-foliated basaltic to andesitic dykes; (b) a second chlorite-rich stage which consists of NNW- to WNW-striking sinistral strike-slip faults and fault-veins temporally and spatially associated with chlorite infills, chlorite-epidote-rich foliated cataclasites with minor amounts of calcite, chlorite-epidote-calcite veins and pseudotachylytes, dominating the core of the Bolfín Fault Zone. This stage corresponds to the first evidence of brittle deformation in the fault zone (Bolfín Fault Zone *sensu-strictu*); (c) an intermediate epidote-rich brittle deformation stage represented by a series of N-, NW- and minor NE-striking faults and fault-veins marked by hydrothermal epidote, quartz and minor calcite precipitation; (4) a later stage, representing the youngest deformation event along the Bolfín Fault Zone, and characterized by NE-striking dextral-normal and N-
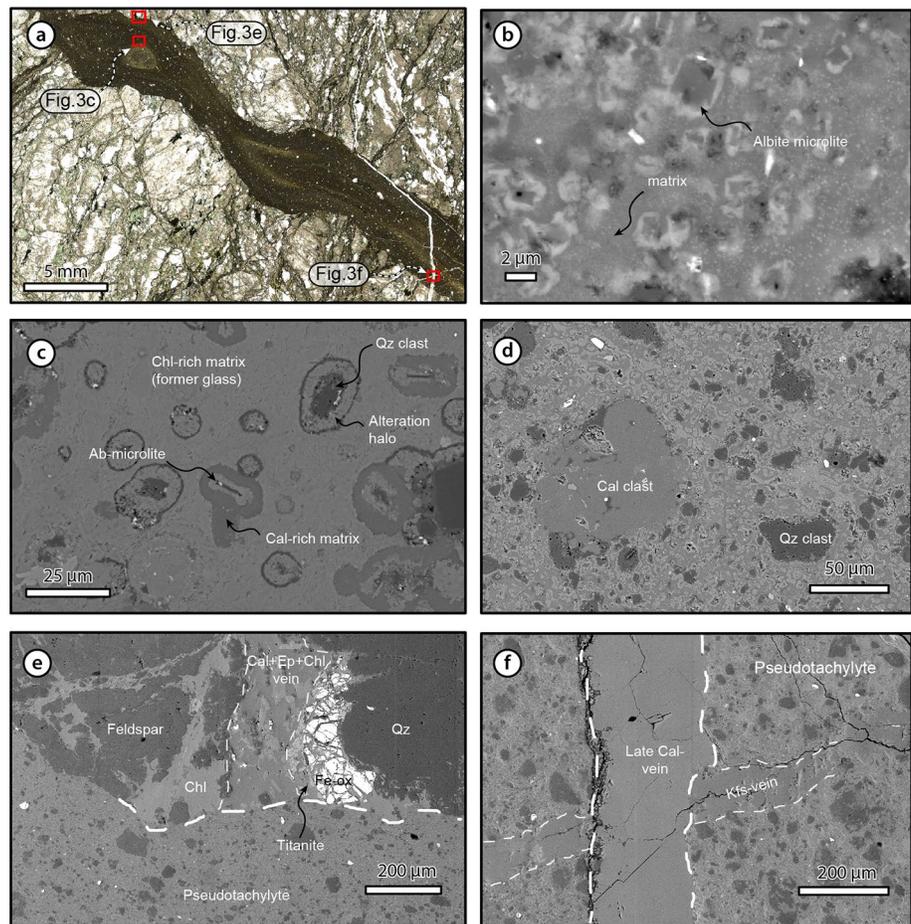
Figure 3. Natural non-vesiculated pseudotachylyte of the Bolfín Fault Zone: evidence for solidification from melt and of seismic faulting in a fluid rich environment. (a) Injection vein (scan of thin section from sample B15-19, parallel nicols) cutting through a chlorite-rich cataclasite. (b) Albite microlites in the pseudotachylyte matrix (sample AT0717). (c) Albite microlites and quartz clasts in a chlorite-rich matrix (presumably devitrified and recrystallized glass; sample B15-19). (d) Calcite and quartz clasts in a microlite-rich pseudotachylyte matrix. (e and f) cross-cutting relations of the natural pseudotachylyte with calcite (early and late) veins and K-feldspar vein. (b–f) BSE-FESEM images. Ab, albite; Qz, quartz; Ep, epidote; Cal, calcite; Chl, chlorite; Kfs, K-feldspar.

and WNW-striking sinistral-normal faults filled with calcite (±gypsum ± palygorskite ± halite). The field evidence suggests the formation of the pseudotachylytes in a fluid-rich environment as discussed below.

5. The Natural Pseudotachylytes of the Bolfín Fault Zone

At Playa Escondida, the exposed Bolfín Fault Zone includes two 1–2 m-thick subvertical fault-core strands spaced apart by 4 m (Figure 1c), containing pseudotachylyte-bearing foliated cataclasites (Figure 2), which merge to the south of the outcrop. The typical occurrence of pseudotachylyte is in several (ca. 20) short and narrow fault-veins, which are generally brown to red while a few are dark gray, ranging in thickness from a few mm to a ca. 3 cm, mostly distributed within the fault-core. In addition to the typical occurrence as fault-veins there are some off-fault injection veins. Almost all the pseudotachylyte fault-veins follow pre-existing structures, such as the magmatic foliation or the "brittle" chlorite-rich faults (Figure 1d). Also, pseudotachylytes veins are altered and dismembered within the fault-core, and are cutting the foliated chlorite-rich cataclasites (Figures 2c and 2d).

At the microscale, two types of pseudotachylytes were recognized: (a) non-vesiculated (Figure 3) and (b) vesiculated pseudotachylytes (Figure 4), both showing flow structures (Figures 3a and 4a), albite microlites
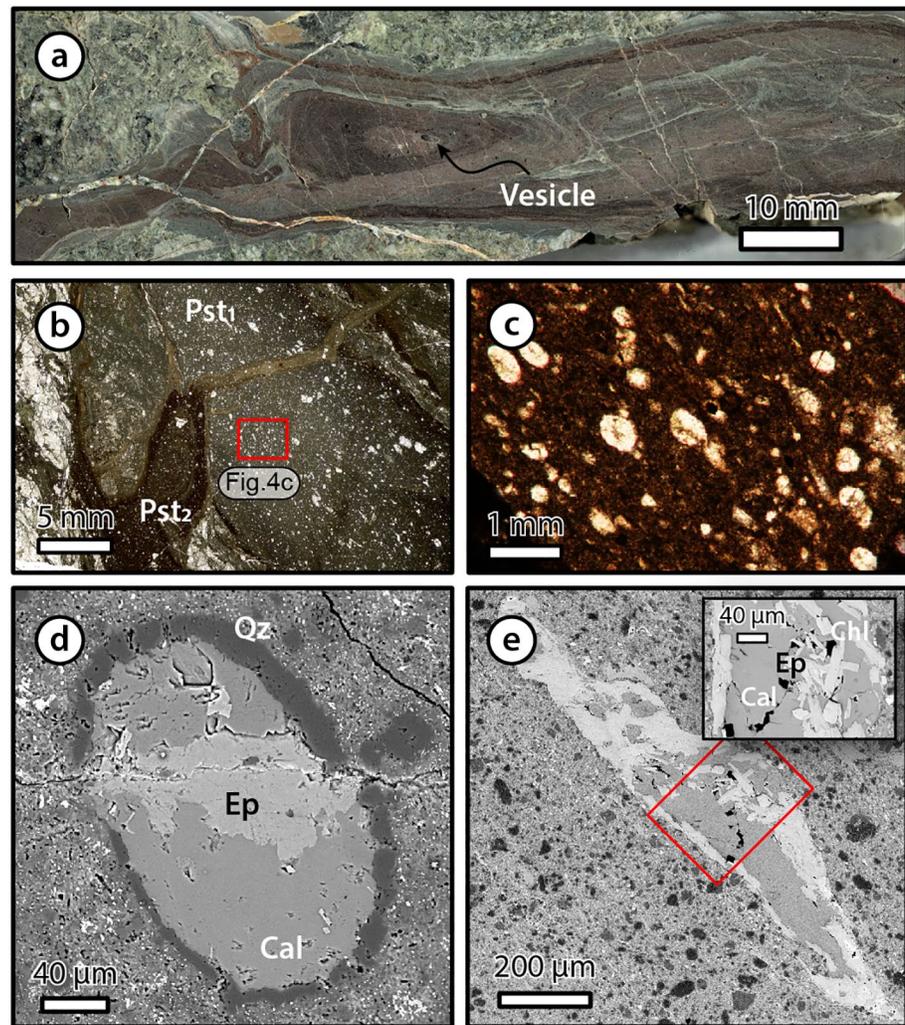
Figure 4. Natural vesiculated pseudotachylyte of the Bolfin Fault Zone: evidence for melt flow and vesiculation. (a) Pseudotachylyte with flow structures and up to 1 mm in size vesicles (scan of polished specimen, sample 2003-01) hosted in a chlorite-rich ultracataclasite. (b) Two generations of pseudotachylytes from sample AT07-2017 (thin section in parallel nicols). The older (Pst_1) is crosscut by the younger and darker (Pst_2). (c) Inset of (b) shows a transmitted light microphotograph of filled vesicles. (d and e) BSE-SEM images of filled vesicles. Qz, quartz; Ep, epidote; Cal, calcite; Chl, chlorite.

(Figures 3b and 3c), chilled margins (Figure 4b) and embayed lithic clasts (Figure 3d), pointing toward their formation from a frictional melt. Vesiculated pseudotachylytes present amygdales (Figure 4) with different shapes and degrees of elongation. In cross section, the amygdales are elliptical (Figure 4d) or have sinuous and irregular contacts with the matrix (Figure 4e). In the latter case, the amygdales are interpreted to be collapsed (Magloughlin, 2011). The matrix of the pseudotachylytes is composed by albite + epidote + Fe-actinolite + chlorite (EMPA analysis, Table S2); whereas the amygdales are filled by calcite + epidote + chlorite + quartz (Figure 4).

Pseudotachylytes, both vesiculated and not vesiculated, cut chlorite and calcite + epidote + chlorite bearing veins (Figure 3e) and are cut by late K-feldspar and calcite veins (Figure 3f). These crosscutting relations indicate that hydrous- and carbonate-rich minerals, associated with hydrothermal alteration were precipitated in the fault zone before, after and possibly during seismic faulting.
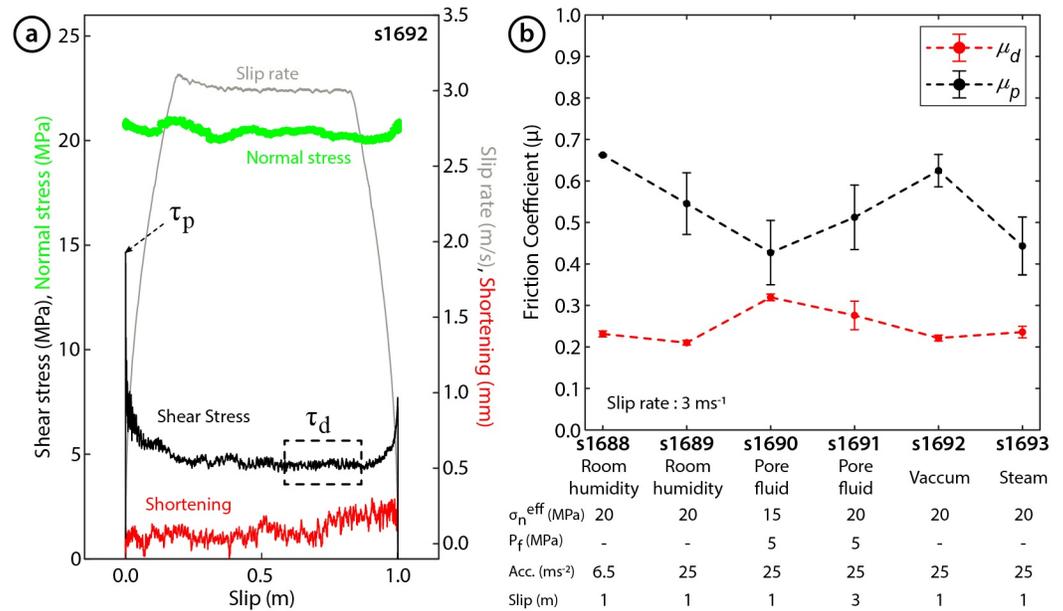
Figure 5. Experimental pseudotachylytes (mechanical data) of SHIVA. (a) Example of the mechanical data (experiment s1692 at vacuum conditions): trapezoidal velocity function (m/s), normal stress (MPa) and obtained shear stress (MPa) and shortening (mm) versus slip distance (m). Peak and dynamic shear stress are shown (τ_p and τ_d, respectively). Dashed black box represents the range of data from which dynamic friction coefficient was estimated. (b) Peak and dynamic friction coefficients (μ_p and μ_d, respectively) graph for all the experiments at different environmental conditions (shown below each experiment name). σ_n^{eff}, Effective normal stress; P_f, Fluid pressure; Acc., Acceleration.

6. Experimental Pseudotachylytes From the Bolfín Fault Zone Rocks

To understand in which environmental conditions vesiculated pseudotachylytes can be produced starting from the Bolfín Fault Zone fault rock assemblage, we performed six high velocity experiments on the two common host-rocks of the natural pseudotachylytes (i.e., the chlorite- and epidote-rich cataclasites). The experiments were performed under vacuum, room humidity, steam and pressurized fluid conditions (see Method section and Figure 5). The sheared fault zone rocks were chlorite- and epidote-rich cataclasites (for the detailed mineralogical assemblage of the sheared rocks, see Figure 8 and Table S3). In these experiments, the frictional evolution with slip was relatively similar and independent of the environmental conditions, loading condition (e.g. Figure 5). In fact, the friction coefficient μ (ratio between the shear stress and the applied effective normal stress; τ/σ_n^{eff}) decayed with slip distance from a peak value of ca. 0.66 at slip initiation, to a dynamic value of ca. 0.25 after ca. 10 cm of slip and (Figure 5). This frictional evolution with slip is typical of cohesive silicate-rich (tonalite, gabbro, peridotite, etc.) experimental faults, also in the presence of pressurized pore fluids (Del Gaudio et al., 2009; Di Toro, Hirose, et al., 2006; Violay, Di Toro, et al., 2015; Violay, Nielsen, et al., 2014). In the presence of pressurized fluids, the dynamic friction value was larger than in the case of vacuum and RH experiments, while on contrary, the peak in shear stress was lower. However, independently of the imposed and environmental conditions, both dynamic and peak friction coefficient were similar (μ_d and μ_p, respectively; Figure 5b). Notably, frictional melts were produced in all the experiments, independent of the presence or absence of pressurized water. The maximum total shortening of the specimens due to rock melting and expulsion of the melt from the slipping zone under these deformation conditions was ca 0.2 mm (Figure S2). The experimental pseudotachylytes were ca. 0.2 mm thick and consisted of plagioclase and quartz "survivor" clasts suspended in a glassy-like matrix (Figure 6). However, the pseudotachylyte at the end of slip (i.e., after 1 m of slip and 3 m of slip for experiment s1691) may not correspond to the total melt produced in the experiment, as a part of this melt was expelled from the slipping zone. The WDS-FESEM composition of the experimental pseudotachylyte matrix (the spot size of the WDS-FESEM analysis was ca. 700 nm in diameter) was homogenous and very similar to the one of a volatile-free basalt, regardless of the environmental conditions imposed in the experiments (Table S3).
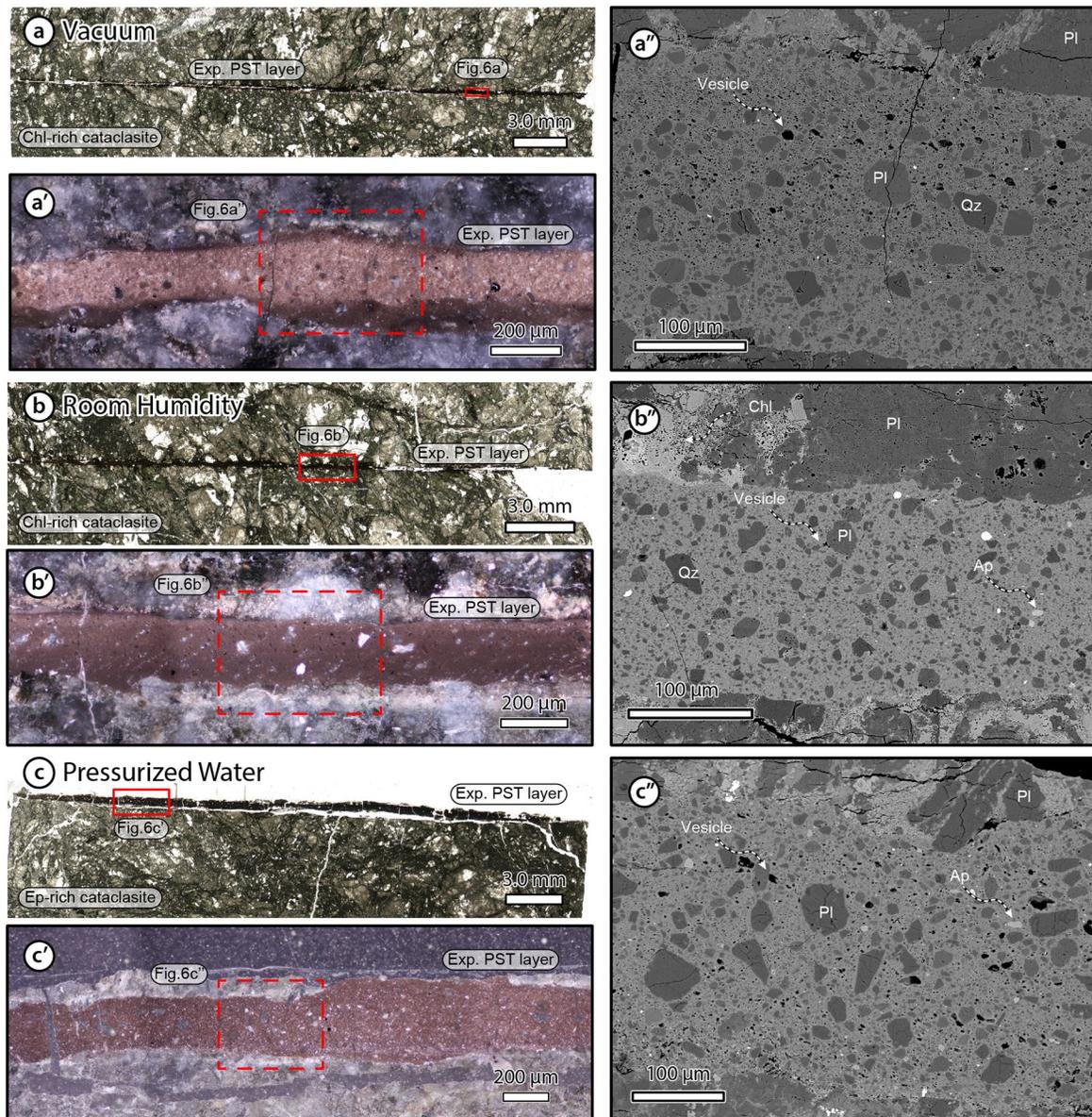
Figure 6. Experimental pseudotachylytes produced under different environmental conditions (a) vacuum, (b) room humidity, and (c) pressurized water. (a–c) Experimental pseudotachylytes layers (Exp. PST layer) and their protolith (both chlorite- and epidote-rich cataclasites; parallel nicols). (a′, b′, c′) Detail of the experimental pseudotachylytes (reflected light). (a″, b″, c″) Vesicles dispersed in the matrix (black dots within the experimental pseudotachylyte layers; for a zoom view of vesicles see Figure 7) were found in all the experimental pseudotachylytes, regardless of the presence or absence of pressurized water at the initiation of slip (BSE-FESEM images). Fragments within the experimental pseudotachylyte layers are mainly quartz (Qz) and plagioclase (Pl). Ap, apatite; Chl, chlorite; Ep, epidote.

Vesicles in experimental pseudotachylytes were found in all the samples, regardless of the imposed environmental conditions, with very similar shape to the amygdales found in the natural pseudotachylytes of Playa Escondida (i.e., both circular to elliptical and collapsed). Vesicles are circular and elliptical in thin section (Figures 7a and 7c), and also with sinuous and irregular contacts with the glassy matrix (Figure 7b). All these shapes are almost identical to those of the natural amygdales (see Figure 4), being the natural ones slightly elongated when compared with the experimental vesicles. The abundance of vesicles is independent of whether free water is present before the experiment. Next to the pseudotachylytes, protolith minerals sometimes are vesiculated and dismembered (Figure 7d).
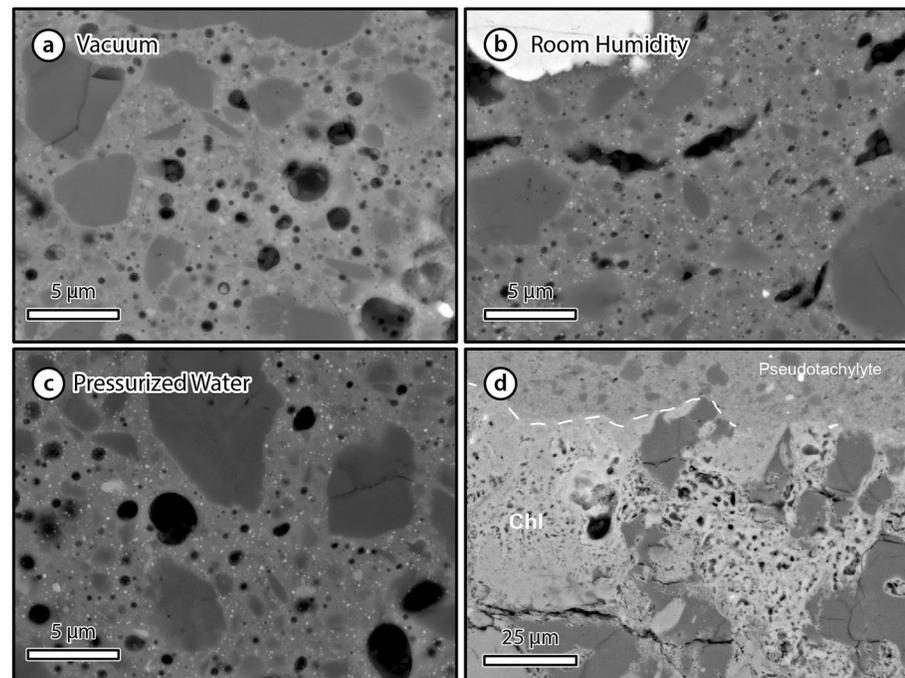
Figure 7. Experimental pseudotachylyte microstructures (BSE-FESEM) at different imposed ambient conditions (a) vacuum, (b) room humidity, (c) 5 MPa fluid pore pressure, and (d) pseudotachylyte – protolith contact (white dashed line). Note the presence of vesicles in the protolith minerals (in this case Chl: chlorite) next to the pseudotachylyte.

7. Mineralogy and Geochemistry

7.1. Mineralogy of Host-Rocks and Natural Pseudotachylytes

X-ray powder diffraction (XRPD) analyses of the fault zone rocks (both host-rock and fault-core), host-rocks of the natural pseudotachylytes (marked with HR after the sample name in Figure 8) and of the protolith of the experimental pseudotachylytes, indicate that the dominant mineral phases are quartz and plagioclase with minor K-feldspar, actinolite and biotite as the mafic phases and titanite as accessory mineral, whereas chlorite, epidote and calcite are the most abundant alteration (hydrous and carbonate) minerals (see Table S4). In contrast, the natural pseudotachylytes (marked with a PST after the sample name in Figure 8), in general, are clearly enriched in K-feldspar and slightly in calcite and biotite and depleted of actinolite when compared to their host-rock. There is a slight broadening of the XRPD spectrum between $20° < 2\theta < 36°$ in the natural pseudotachylyte when compared with adjacent host rock (see Figure S3). Though broadening of the XRPD spectrum has been interpreted as due to the presence of glass (e.g., Lin & Shimamoto, 1998), the presence of glass in the Bolfín pseudotachylyte is unlikely because of the intense chlorite-epidote alteration. Another possibility of the slight broadening could be due to remnants of nanomaterial within the pseudotachylytes formed during melt solidification.

7.2. Elemental Composition of Experimental Pseudotachylytes

EMPA and FESEM-WDS investigations of the glassy matrix of experimental pseudotachylytes gave very similar results, despite their different spot size (ca. 3 μm for EMPA, ca. 0.7 μm for FESEM-WDS). Moreover, the compositions of glass in samples produced in different ambient conditions (vacuum for experiment s1692, room humidity for experiment s1688 and pressurized pore water for experiment s1690) are indistinguishable (Figure 9). The composition of the experimental glass (ca. 49.9% SiO_2, 17.0% Al_2O_3, 10.8% FeO, 8.2% CaO, 5.2% MgO, 2.7 Na_2O, 1.5% TiO_2, and 1.0% K_2O) corresponds to the one of a basalt (e.g., Papale et al., 2006).
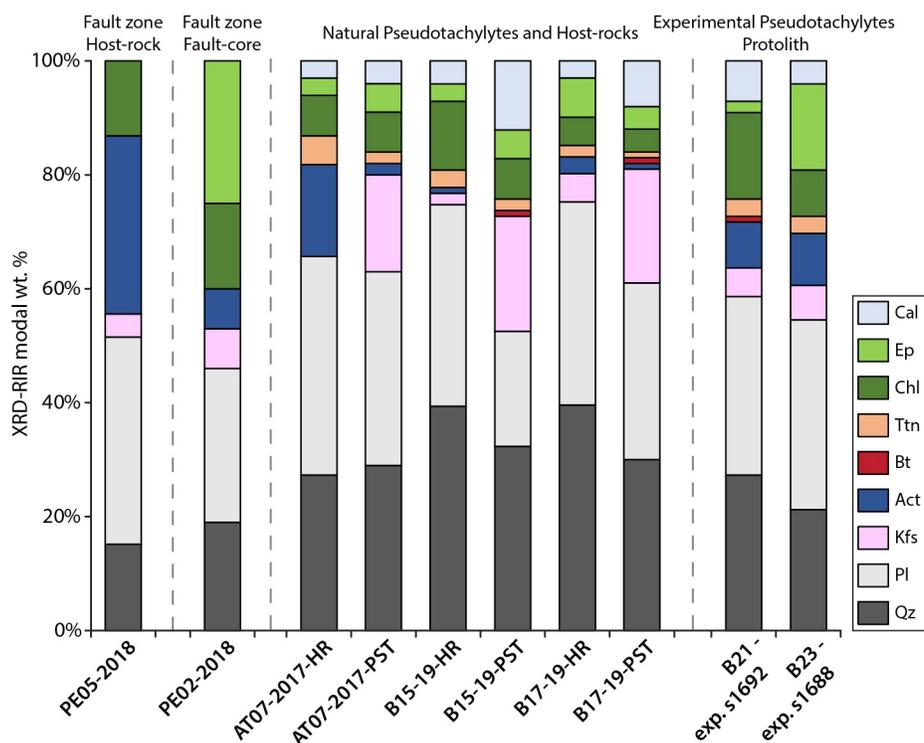
Figure 8. Mineralogical compositions (XRD semi-quantitative analysis) of the Bolfín Fault Zone host-rock and fault-core, natural pseudotachylytes (including their host rocks) and of the protolith sheared with SHIVA to produce experimental pseudotachylytes (B21: chlorite-rich, for experiment s1692, and B23: epidote-rich for experiment s1688). Cal, calcite; Ep, epidote; Chl, chlorite; Ttn, titanite; Bt, biotite; Act, actinolite; Kfs, K-feldspar; Pl, Plagioclase; Qz, Quartz.

8. Discussion

8.1. Formation of Pseudotachylytes in Fluid-Rich Conditions

It is commonly considered that pseudotachylytes mainly form during seismic slip under dry conditions (Sibson & Toy, 2006), as the presence of free pore fluid would reduce the normal effective stress during thermal pressurization in the slipping zone before friction melt is generated (Rice, 2006; Sibson, 1975). Recent work has shown that the effectiveness of this melt-limiting pressurization also depends of the permeability and storage capacity of the damaged wall rock adjacent to the slip zone (Brantut & Mitchell, 2018). However, we document compelling evidence of natural pseudotachylyte formed in a hydrothermal fluid-rich environment (i.e., the volume of fluid-rich fault rocks containing (a) free pore water or (b) volatile-rich minerals) supported by the presence of chlorite + epidote + calcite veins and K-feldspar and calcite veins that pre- and post-date the generation of the natural pseudotachylytes.

The presence of amygdales has already been proposed as a key characteristic of fluid-rich pseudotachylyte melts (e.g., Maddock et al., 1987; Magloughlin, 2011) and inferred to be the result of the degassing of a vapor phase from the silicate melt (Kirkpatrick & Rowe, 2013). Moreover, rotary shear experiments provided evidence that frictional melts can be easily produced during seismic slip in the presence of pressurized water (Spray, 1995; Violay, Di Toro, et al., 2015; Violay, Nielsen, et al., 2014). In turn, our experiments showed that vesicles, under these unconfined experimental conditions, may form regardless of the presence of free pore water at slip initiation (Figure 7), as also reported by Violay, Nielsen, et al. (2014) and Violay, Di Toro, et al. (2015), for both conditions, and by several authors for dry experiments (e.g. Fondriest et al., 2020; Han et al., 2014; Mittempergher et al., 2014; Ujiie, Tsutsumi, et al., 2009). This experimental evidence points toward the possibility that volatiles (and, as a consequence, their separation from the frictional melt and the formation of vesicles) could have originated by two (not mutually exclusive) mechanisms: (a) the breakdown and release of volatiles from hydrous- and carbonate-bearing minerals—in the case of the Bolfín
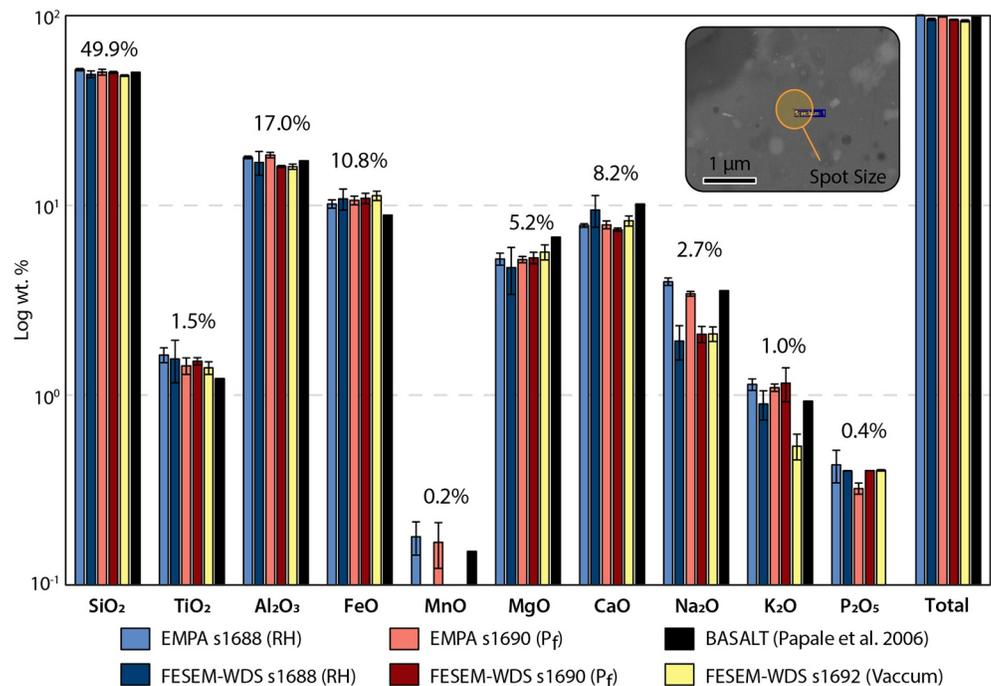
Figure 9. Elemental analyses (EMPA and FESEM-WDS) of experimental pseudotachylytes formed at different conditions: RH, Room Humidity; Vac, vacuum; P_f, pore pressure (H_2O = 5 MPa). The elemental compositions of the experimental glass are compared with those of a common basalt (black in color columns, from Papale et al., 2006). The reported wt.% are the average of 4–6 points analyses (see Table S3). Beam spot size is marked in the inset.

Fault Zone natural pseudotachylytes from Playa Escondida: chlorite, calcite, epidote and actinolite—and (b) the presence of free pore water before seismic slip. Unfortunately, based on the geochemical evidence presented here and the intense chlorite-epidote alteration of the natural pseudotachylytes and both their host-rock and protolith, we are not able to discern between the two mechanisms. However, in this study we report the presence of vesicles in both natural rocks (as well as amygdales) and laboratory samples, thus indicating that even in the presence of pressurized and free pore water (i.e., case for the experimental pseudotachylytes) frictional melting can easily occur during seismic slip. The field and petrographic evidences indicate that the pseudotachylytes in the Bolfin Fault Zone were formed by seismic slip during a period of hydrothermal activity. Moreover, the subsequent mineralogical and experimental results indicate that seismic melting under water saturated conditions is possible for the rock and mineral alteration observed in the fault. It is still possible that the fault could have been dried out just before the initiation of the seismic activity and that melting occurred in dry conditions. However, this is less probable and there is no evidence for such a change.

8.2. Composition of the Friction Melt at the Time of Ancient Seismic Faulting

Degassing of volatiles (and formation of vesicles) from silicate melts is controlled by melt temperature and composition, amount of volatiles and confining pressure (Papale et al., 2006; Shishkina et al., 2010). Because the vesiculated and non-vesiculated natural pseudotachylytes are intensively altered, it is not possible to determine the glass (and infer the melt) composition at the time of seismic faulting. But the natural pseudotachylytes, based on cross-cutting relationships, are the result of frictional melting of altered rocks similar, if not identical, in composition to those sheared with SHIVA in the laboratory. As a consequence, we assumed that the composition of the solidified friction melt (=glass) before alteration was similar in composition to the glass (and to the melt) produced in our experiments (Figure 9). It is significant to note that the composition of the two experimental glasses is very similar, if not identical, and is independent of the imposed environmental conditions (room humidity, pressurized H_2O or vacuum) and corresponds to that of a basalt (Figure 9 and Table S3).
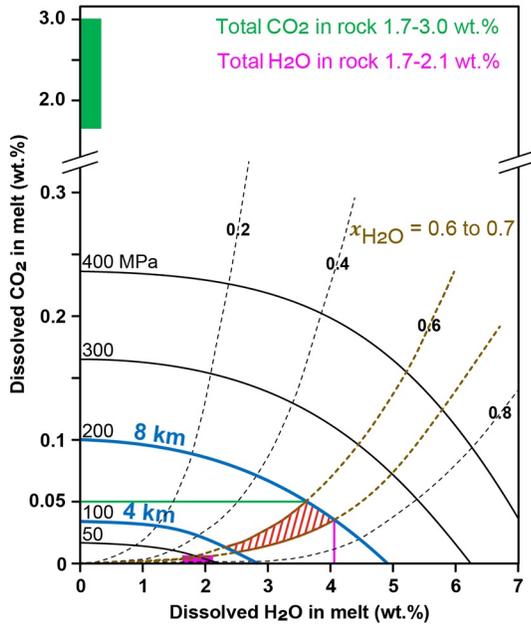
Figure 10. Solubility graph for H_2O and CO_2 in a basaltic in composition melt at 1,200°C (after Shishkina et al., 2010). The diagram reports the dissolved wt.% of H_2O and CO_2 in a basaltic melt. The continuous curves are the confining pressures (in blue are reported the estimated depth of formation of the pseudotachylytes from Playa Escondida) and the dashed curves are the estimated mole fraction of x_{H_2O} at the time of seismic faulting (Equation 4). The red-dashed area is the admissible natural condition of solubility for the pseudotachylytes from Playa Escondida, whereas the pink and green colored areas represent the saturation conditions of dissolved H_2O and CO_2, respectively, in a basaltic melt at 1,200°C. Importantly, CO_2 is almost immiscible in basaltic melts: the green area is located to the top left where the confining pressures should be of the order of several GPa (note the change in scale of the ordinate axis) to allow the dissolution of CO_2 in the melt. Because of the quite common presence of chlorite-epidote-calcite-bearing veins in the host-rocks and their breakdown with release of CO_2 during frictional heating associated with seismic slip, the formation of vesicles was almost inevitable in the friction melts (now pseudotachylytes) from Playa Escondida.

8.3. Water and Carbonate Vesiculation

In the experiments, the total amount of volatiles available during frictional melting can be estimated based on the amount of H_2O- and CO_2-bearing minerals in the protolith (Equation 1; e.g., $[Chl]_{HR}$ = 15% wt. in sample; see XRD analysis, Figure 8 and Table S4) and in their respective volatile content (e.g. $[H_2O]_{Chl}$ = 12 wt.% H_2O see Tables S4 and S5, after Deer et al. [2013] and Di Toro & Pennacchioni [2004]):

$$\%\text{wt. volatiles} = \frac{1}{100} \sum_{min\_1}^{min\_i} [\text{volatiles}]_{min\_i} [\text{Min}]_{HR} \quad (1)$$

$$\%\text{wt. } H_2O = \frac{1}{100} \{ [H_2O]_{Chl}[Chl]_{HR} + [H_2O]_{Ep}[Ep]_{HR} \\ + [H_2O]_{Fe-act}[Fe-act]_{HR} + [H_2O]_{Bt}[Bt]_{HR} \} \quad (2)$$

$$\%\text{wt. } CO_2 = \frac{1}{100}[CO_2]_{Cc}[Cc]_{HR} \quad (3)$$

Based on Equations 2 and 3, in the experimentally sheared samples, the %wt. H_2O and %wt. CO_2 can be calculated for the experimentally sheared protolith samples. %wt. H_2O ranges from 1.68 (sample B23) to 2.11 (sample B21) and the %wt. CO_2 from 1.74 (sample B23) to 3.04 (sample B21). This estimation assumes that both hydrous- and carbonate-rich minerals where all precipitated prior to frictional melting, even though there is evidence for late fluid circulation as attested by calcite veins cross-cutting through the natural pseudotachylytes (Figure 3f). Consequently, they must be considered as maximum values of %wt. H_2O and CO_2.

What is the fate of these volatiles in a basaltic-in-composition friction melt (EMPA and FESEM-WDS analysis)? The solubility of two component, H_2O-CO_2, fluids in basaltic melts varies depending on molar fraction of the fluid, confining pressure and melt temperature. Assuming total melting of chlorite, epidote, Fe-actinolite and calcite, the mole fractions x for H_2O and CO_2 are:

$$x_{H_2O} = \frac{n_{H_2O}}{n_{H_2O} + n_{CO_2}} \text{ and } x_{CO_2} = 1 - x_{H_2O} \quad (4)$$

Experimental and theoretical studies showed that under equilibrium conditions, the solubility of CO_2 is up to one order of magnitude lower than for H_2O in basaltic melts (Papale et al., 2006; Shishkina et al., 2010). In particular, under the experimental conditions investigated here (maximum fluid pressure limited to 5 MPa, and a maximum total normal stress of 20 MPa), volatiles (both H_2O and CO_2) are virtually immiscible in silicate melts (Wallace et al., 2015) and it is not surprising to find empty vesicles in the experimental pseudotachylytes (Figure 6). However, in the case of the natural pseudotachylytes produced between 4 and 8 km depth, confining pressures can be up to 200 MPa and hydrostatic pore pressure will be 60–80 MPa, and potentially much higher. Under these effective confining pressures and assuming thermodynamic equilibrium, constant fluid composition and temperature, volatiles dissolve in the melt. In particular, at T = 1,200°C (a reasonable temperature for these friction melts) a two component H_2O-CO_2 fluid with x_{H_2O} = 0.6–0.7 (as in the case of samples B21-B23) may dissolve in a basaltic melt up-to 2.3–4.1%wt. H_2O and up-to 0.025–0.05%wt. CO_2 from 100 to 200 MPa, respectively (Figure 10; combination of theoretical estimates and experimental measures of H_2O and CO_2 solubility in basaltic melts, see Figure 12b in Papale et al. [2006] and Figure 6 in Shishkina et al. [2010]). Because the maximum wt.% H_2O content available in the melt might be up to 2.11%, the presence of amygdales (i.e., filled vesicles, see Figure 4) may suggest either (a) that the pseudotachylytes were produced under very shallow conditions or (b) that there were free pore fluids in

the slipping zone. However, microstructural evidence from the calcite veins truncated by the pseudotachylytes (Figure 3e), and calcite clasts included in the pseudotachylyte (Figure 3d), suggest that breakdown of calcite occurred during seismic faulting. Given the very limited solubility of CO_2 in basaltic melts, the formation of CO_2 bubbles during frictional melting was expected. A similar result was obtained by studying fluid inclusions in pseudotachylytes of the Noijima fault (Famin et al., 2008). As a matter of fact, though the composition of the altered tonalite is quite similar, and so is the H_2O content, the pseudotachylytes found at Playa Escondida have a widely varying vesicle content. We speculate that the presence of vesicles is related to the presence of nearby (i.e., few cm away) calcite veins truncated by the pseudotachylyte. The implication is that H_2O was completely dissolved in the melt and, due to the highly altered nature of the rock, that there is no possibility to our knowledge to show whether or not the frictional melt formed in the presence of H_2O-rich pore fluids.

8.4. Brittle Overprinting and Alteration of Pseudotachylytes

The pseudotachylytes of the Playa Escondida outcrop are found principally in the fault-core, cutting foliated cataclasites (chlorite-rich) and some are dismembered and much more altered within the cataclastic rocks (Figures 2c and 2d). The mineralogy of the pseudotachylytes consists mainly of quartz and plagioclase, which can be found as un-melted clasts and recrystallized microlites within the matrix, respectively (Figure 3). Also they are enriched in K-feldspar and slightly in calcite (both observed as late veins cutting the pseudotachylytes and as alteration products of the matrix), and biotite and depleted of actinolite when compared to their contact host-rock (Figures 3 and 8), while chlorite is mostly found as an alteration product of the pseudotachylyte matrix (former glass in Figure 3c). This alteration mineral assemblage is characteristic of a (sub-) greenschist facies condition. The observed amygdales are mainly filled by calcite, epidote, chlorite and minor quartz (Figure 3), which clearly imply post-seismic fluid percolation through the pseudotachylyte matrix (Figure 4). Hence, the natural pseudotachylytes were produced by the melting of hydrous- and carbonate-rich minerals during seismic faulting, most likely under the presence of infiltrated hydrothermal fluids, giving to the pseudotachylytes (both natural and experimental) a dark gray and brownish-red color (Figures 2c, 2d, and 6), where in the field the brownish-red correspond to the oldest, most altered ones that resemble a cataclastic rock (either a cataclasite or an ultracataclasite), making them hard to distinguish.

Experimental evidence testing the preservation potential of pseudotachylyte's primary microtextures in the presence of hydrothermal fluids ($P_p \geq 150$ MPa, $T \geq 300°C$), documents their rapid (days to months) alteration (Fondriest et al., 2020). Experimental pseudotachylytes were heavily altered with dissolution of the matrix, neo-formation of clay aggregates and generation of a clastic microtexture (Fondriest et al., 2020). The alteration of pseudotachylytes driven by hydrothermal fluids is consistent with earthquake faulting being responsible for the rapid infiltration and redistribution of large volumes of fluids in the upper crust (Sibson, 1981) and the generation of hydrothermal mineralization; a condition which *sensu lato* can apply to the Bolfin Fault Zone case.

Pseudotachylytes can be intrinsically difficult to identify in fault zones, because they are ultrafine-grained dark colored rocks, often very thin, and spatially associated or overprinted by other macroscopically similar fault products such as ultracataclasites and ultramylonites (Kirkpatrick & Rowe, 2013). As a result, the potential rapid alteration of pseudotachylytes by hydrothermal fluids can further hamper the identification of pseudotachylyte in natural fault zones. Pseudotachylytes, therefore, may be largely under-reported in the geological record, thus leading to a biased evaluation of frictional melting as a relevant on-fault co-seismic process.

9. Conclusions

Tectonic pseudotachylytes are thought to be rare in the geological record because they are either rarely produced, rarely preserved or both (Kirkpatrick & Rowe, 2013; Sibson, 1975). Moreover, some authors hold that pseudotachylytes are thought not to be produced in fluid-rich (especially water-rich) environments (Sibson & Toy, 2006). In this view, the formation of frictional melts should be hampered by (a) the heat adsorbed by water which would buffer the temperature increase in the fault-core and (b) the thermal expansion of water, which would lead to fault dynamic weakening by thermal pressurization before bulk frictional melting may

occur (Rice, 2006; Sibson, 1973). However, from our observations of both natural and experimental pseudotachylytes we conclude the following:

- In the Bolfín Fault Zone, a ca. 45 km-long strike-slip fault segment of the ca. 1,000 km-long Atacama Fault System (Chile), and capable of having produced > *M* 6.0 earthquakes, we found pseudotachylytes produced in a hydrothermal fluid-rich environment (Figures 2 and 3). These pseudotachylytes, which are hosted in the continental crystalline basement of the Coastal Cordillera, are, to our knowledge, the first pseudotachylytes described in the Chilean Andes, giving hints that they could be more common than previously thought even in this tectonic setting.
- Although there is ample evidence for fluid-rock interaction during ancient seismic faulting along the Bolfín Fault Zone (Figures 2, 3, and 8), unfortunately, we could not demonstrate if pressurized water was present or not at the exact moment of friction melting.
- Experiments reproducing seismic slip conditions and performed on the altered host-rocks of the natural pseudotachylytes from Playa Escondida (Figure 8), confirm that frictional melts can form in the presence of pressurized water (Figures 6 and 7). Moreover, the experiments suggest that the primary composition of the matrix of the pseudotachylytes from Playa Escondida was similar to the composition of a basalt (Figure 9). This primary composition of natural pseudotachylytes was then altered as more fluids percolated through the fault zone.
- Several pseudotachylyte fault-veins from Playa Escondida include amygdales in their matrix (Figure 4). The amygdales are interpreted as the result of degassing and vesiculation of H_2O and CO_2 in the friction melt (Figure 10) and later post-seismic filling (quartz, epidote, chlorite, calcite) from percolating fluids during post-seismic fault healing or in situ alteration (Figure 4). The two main volatile species (H_2O and CO_2) can be produced by the break-down of water- (chlorite, epidote, actinolite and biotite) and carbonate-bearing minerals (i.e., calcite) during frictional heating associated with seismic slip (this is confirmed by the experiments conducted under vacuum conditions, Figure 7) or may be already present in the pores of the fault-core before seismic slip.
- CO_2 has an extremely low miscibility in basaltic melts at any given effective confining pressure and temperature with respect to H_2O (Figure 10). We suggest that the occurrence of vesicles (now amygdales) in the matrix of the pseudotachylytes from Playa Escondida (amygdales were found only in some pseudotachylytes, though the composition of the altered host-rocks is quite homogeneous and always includes epidote and chlorite, Figure 8) is probably related to the nearby presence of calcite-bearing veins cut by the pseudotachylyte-bearing fault.
- In hydrothermal fluid-rich environments, as the one found in Playa Escondida evidenced by the presence of volatile-rich minerals (hydrous and carbonate minerals) and veins, pseudotachylytes are prone to alteration and are easily lost from the geological record.

Based on this evidence, we conclude that frictional melting can easily occur in fluid-rich fault zones as well as in the presence of pressurized pore fluids according to what our experiments indicate. This implies that pseudotachylytes might be more common than usually thought and, as a consequence, melt lubrication could be considered one of the most efficient seismic dynamic weakening mechanisms in the basement rocks of the continental crust.

Data Availability Statement

The field structural data, the mechanical data of the experiments and EMPA, FESEM-WDS and XRD analyses and volatile calculations are available in the Mendeley Data Repository under http://dx.doi.org/10.17632/kkbkfwtgbd.1.

References

Allen, A. R. (1979). Mechanism of frictional fusion in fault zones. *Journal of Structural Geology*, *1*(3), 231–243. https://doi.org/10.1016/0191-8141(79)90042-7

Arabasz, W. J. (1971). Geological and geophysical studies of the Atacama fault zone in northern Chile (Vol. 1971). California Institute of Technology.

Arancibia, G., Fujita, K., Hoshino, K., Mitchell, T. M., Cembrano, J., Gomila, R., et al. (2014). Hydrothermal alteration in an exhumed crustal fault zone: Testing geochemical mobility in the Caleta Coloso Fault, Atacama Fault System, Northern Chile. *Tectonophysics*, *623*, 147–168. https://doi.org/10.1016/j.tecto.2014.03.024

Bjørnerud, M. (2010). Rethinking conditions necessary for pseudotachylyte formation: Observations from the Otago schists, South Island, New Zealand. *Tectonophysics*, *490*(1–2), 69–80. https://doi.org/10.1016/j.tecto.2010.04.028

Boullier, A., Ohtani, T., Fujimoto, K., Ito, H., & Dubois, M. (2001). Fluid inclusions in pseudotachylytes from the Nojima fault, Japan. *Journal of Geophysical Research: Solid Earth*, *106*(B10), 21965–21977. https://doi.org/10.1029/2000JB000043

Brantut, N., & Mitchell, T. M. (2018). Assessing the efficiency of thermal pressurization using natural pseudotachylyte-bearing rocks. *Geophysical Research Letters*, *45*(18), 9533–9541. https://doi.org/10.1029/2018GL078649

Cembrano, J., González, G., Arancibia, G., Ahumada, I., Olivares, V., & Herrera, V. (2005). Fault zone development and strain partitioning in an extensional strike-slip duplex: A case study from the Mesozoic Atacama fault system, Northern Chile. *Tectonophysics*, *400*(1–4), 105–125. https://doi.org/10.1016/j.tecto.2005.02.012

Cowan, D. S. (1999). Do faults preserve a record of seismic slip? A field geologist's opinion. *Journal of Structural Geology*, *21*, 995–1001. https://doi.org/10.1016/s0191-8141(99)00046-2

Deer, W. A., Howie, R. A., & Zussman, J. (2013). An introduction to the rock-forming minerals (Vol. 20). Mineralogical Society of Great Britain and Ireland. https://doi.org/10.1180/DHZ

Del Gaudio, P., Di Toro, G., Han, R., Hirose, T., Nielsen, S., Shimamoto, T., & Cavallo, A. (2009). Frictional melting of peridotite and seismic slip. *Journal of Geophysical Research*, *114*(B6). https://doi.org/10.1029/2008jb005990

Di Toro, G., Hirose, T., Nielsen, S., Pennacchioni, G., & Shimamoto, T. (2006). Natural and experimental evidence of melt lubrication of faults during earthquakes. *Science*, *311*(5761), 647–649. https://doi.org/10.1126/science.1121012

Di Toro, G., Niemeijer, A., Tripoli, A., Nielsen, S., Di Felice, F., Scarlato, P., et al. (2010). From field geology to earthquake simulation: A new state-of-The-art tool to investigate rock friction during the seismic cycle (SHIVA). *Rendiconti Lincei*, *21*(1), 95–114. https://doi.org/10.1007/s12210-010-0097-x

Di Toro, G., & Pennacchioni, G. (2004). Superheated friction-induced melts in zoned pseudotachylytes within the Adamello tonalites (Italian Southern Alps). *Journal of Structural Geology*, *26*(10), 1783–1801. https://doi.org/10.1016/j.jsg.2004.03.001

Dixon, J. E., & Dixon, T. H. (1987). Vesicles, amygdales and similar structures in fault-generated pseudotachylytes - Comment. *Lithos*, *23*(5), 225–229. https://doi.org/10.1016/0024-4937(87)90019-3

Famin, V., Nakashima, S., Boullier, A.-M., Fujimoto, K., & Hirono, T. (2008). Earthquakes produce carbon dioxide in crustal faults. *Earth and Planetary Science Letters*, *265*(3–4), 487–497. https://doi.org/10.1016/j.epsl.2007.10.041

Fondriest, M., Mecklenburgh, J., Passelegue, F. X., Artioli, G., Nestola, F., Spagnuolo, E., et al. (2020). Pseudotachylyte alteration and the rapid fade of earthquake scars from the geological record. *Geophysical Research Letters*, *47*(22). https://doi.org/10.1029/2020GL090020

Gomila, R., Arancibia, G., Mitchell, T. M., Cembrano, J. M., & Faulkner, D. R. (2016). Palaeopermeability structure within fault-damage zones: A snap-shot from microfracture analyses in a strike-slip system. *Journal of Structural Geology*, *83*, 103–120. https://doi.org/10.1016/j.jsg.2015.12.002

González, G. (1999). Mecanismo y profundidad de emplazamiento del Plutón de Cerro Cristales, Cordillera de la Costa, Antofagasta, Chile. *Revista Geológica de Chile*, *26*(1), 43–56. https://doi.org/10.4067/S0716-02081999000100003

González, G., & Niemeyer, H. (2005). Cartas Antofagasta y Punta Tetas, Región Antofagasta. Servicio Nacional de Geología y Minería, Carta Geológica de Chile, Serie Geología Básica (Vol. 89, p. 35). escala 1:100.000.

Han, R., Hirose, T., Jeong, G. Y., Ando, J., & Mukoyoshi, H. (2014). Frictional melting of clayey gouge during seismic fault slip: Experimental observation and implications. *Geophysical Research Letters*, *41*(15), 5457–5466. https://doi.org/10.1002/2014GL061246

Herrera, V., Cembrano, J., Olivares, V., Kojima, S., & Arancibia, G. (2005). Precipitación por despresurización y ebullición en vetas hospedadas en un dúplex de rumbo extensional: Evidencias microestructurales y microtermométricas. *Revista Geológica de Chile*, *32*(2), 207–227. https://doi.org/10.4067/S0716-02082005000200003

Jensen, E., Cembrano, J., Faulkner, D., Veloso, E., & Arancibia, G. (2011). Development of a self-similar strike-slip duplex system in the Atacama Fault system, Chile. *Journal of Structural Geology*, *33*(11), 1611–1626. https://doi.org/10.1016/j.jsg.2011.09.002

Kirkpatrick, J. D., & Rowe, C. D. (2013). Disappearing ink: How pseudotachylytes are lost from the rock record. *Journal of Structural Geology*, *52*(1), 183–198. https://doi.org/10.1016/j.jsg.2013.03.003

Lachenbruch, A. H. (1980). Frictional heating, fluid pressure, and the resistance to fault motion. *Journal of Geophysical Research: Solid Earth*, *85*(B11), 6097–6112. https://doi.org/10.1029/JB085iB11p06097

Lee, S. K., Han, R., Kim, E. J., Jeong, G. Y., Khim, H., & Hirose, T. (2017). Quasi-equilibrium melting of quartzite upon extreme friction. *Nature Geoscience*, *10*(6), 436–441. https://doi.org/10.1038/ngeo2951

Lin, A., & Shimamoto, T. (1998). Selective melting processes as inferred from experimentally generated pseudotachylytes. *Journal of Asian Earth Sciences*, *16*(5–6), 533–545. https://doi.org/10.1016/S0743-9547(98)00040-3

Maddock, R. H. (1983). Melt origin of fault-generated pseudotachylytes demonstrated by textures. *Geology*, *11*(2), 105–108. https://doi.org/10.1130/0091-7613(1983)11<105:MOOFPD>2.0.CO;2

Maddock, R. H. (1992). Effects of lithology, cataclasis and melting on the composition of fault-generated pseudotachylytes in Lewisian gneiss, Scotland. *Tectonophysics*, *204*(3–4), 261–278. https://doi.org/10.1016/0040-1951(92)90311-S

Maddock, R. H., Grocott, J., & Van Nes, M. (1987). Vesicles, amygdales and similar structures in fault-generated pseudotachylytes. *Lithos*, *20*(5), 419–432. https://doi.org/10.1016/0024-4937(87)90019-3

Maddock, R. H., Grocott, J., & Van Nes, M. (1989). Vesicles, amygdales and similar structures in fault-generated pseudotachylytes - Reply. *Lithos*, *23*, 227–229. https://doi.org/10.1016/0024-4937(89)90008-x

Magloughlin, J. F. (1989). The nature and significance of pseudotachylite from the Nason terrane, North Cascade Mountains, Washington. *Journal of Structural Geology*, *11*(7), 907–917. https://doi.org/10.1016/0191-8141(89)90107-7

Magloughlin, J. F. (1992). Microstructural and chemical changes associated with cataclasis and frictional melting at shallow crustal levels: The cataclasite-pseudotachylyte connection. *Tectonophysics*, *204*(3–4), 243–260. https://doi.org/10.1016/0040-1951(92)90310-3

Magloughlin, J. F. (2011). Bubble collapse structure: A microstructural record of fluids, bubble formation and collapse, and mineralization in pseudotachylyte. *The Journal of Geology*, *119*(4), 351–371. https://doi.org/10.1086/659143

Magloughlin, J. F., & Spray, J. G. (1992). Frictional melting processes and products in geological materials: Introduction and discussion. *Tectonophysics*, *204*(3–4), 197–204. https://doi.org/10.1016/0040-1951(92)90307-R

Meneghini, F., Di Toro, G., Rowe, C. D., Moore, J. C., Tsutsumi, A., & Yamaguchi, A. (2010). Record of mega-earthquakes in subduction thrusts: The black fault rocks of Pasagshak Point (Kodiak Island, Alaska). *Bulletin of the Geological Society of America*, *122*(7–8), 1280–1297. https://doi.org/10.1130/B30049.1

Mittempergher, S., Dallai, L., Pennacchioni, G., Renard, F., & Di Toro, G. (2014). Origin of hydrous fluids at seismogenic depth: Constraints from natural and experimental fault rocks. *Earth and Planetary Science Letters*, *385*, 97–109. https://doi.org/10.1016/j.epsl.2013.10.027

Nielsen, S., Di Toro, G., Hirose, T., & Shimamoto, T. (2008). Frictional melt and seismic slip. *Journal of Geophysical Research: Solid Earth*, *113*(1). https://doi.org/10.1029/2007JB005122

Niemeijer, A., Di Toro, G., Nielsen, S., & Di Felice, F. (2011). Frictional melting of gabbro under extreme experimental conditions of normal stress, acceleration, and sliding velocity. *Journal of Geophysical Research: Solid Earth*, *116*(7), 1–18. https://doi.org/10.1029/2010JB008181

Nockolds, S. R. (1940). Petrology of rocks from Queen Mary Land. *Australasian Antarctic Expedition, 1911–14*. Scientific Reports, Series A (Vol. 4, pp. 15–86).

Olivares, V., Cembrano, J., Arancibia, G., Reyes, N., Herrera, V., & Faulkner, D. (2010). Significado tectónico y migración de fluidos hidrotermales en una red de fallas y vetas de un Duplex de rumbo: Un ejemplo del Sistema de Falla de Atacama. *Andean Geology*, *37*(2), 473–497. https://doi.org/10.5027/andgeov37n2-a12

Papale, P., Moretti, R., & Barbato, D. (2006). The compositional dependence of the saturation surface of $H_2O + CO_2$ fluids in silicate melts. *Chemical Geology*, *229*(1–3), 78–95. https://doi.org/10.1016/j.chemgeo.2006.01.013

Phillips, N. J., Rowe, C. D., & Ujiie, K. (2019). For how long are pseudotachylytes strong? Rapid alteration of basalt-hosted pseudotachylytes from a shallow subduction complex. *Earth and Planetary Science Letters*, *518*, 108–115. https://doi.org/10.1016/j.epsl.2019.04.033

Philpotts, A. R. (1964). Origin of pseudotachylites. *American Journal of Science*, *262*(8), 1008–1035. https://doi.org/10.2475/ajs.262.8.1008

Pirajno, F. (2009).Water and hydrothermal fluids on Earth. In *Hydrothermal processes and mineral systems* (pp. 1–71). Springer Netherlands. https://doi.org/10.1007/978-1-4020-8613-7_1

Rice, J. R. (2006). Heating and weakening of faults during earthquake slip. *Journal of Geophysical Research: Solid Earth*, *111*(B5). https://doi.org/10.1029/2005JB004006

Rowe, C. D., & Griffith, W. A. (2015). Do faults preserve a record of seismic slip: A second opinion. *Journal of Structural Geology*, *78*, 1–26. https://doi.org/10.1016/j.jsg.2015.06.006

Rowe, C. D., Moore, J. C., Meneghini, F., & McKeirnan, A. W. (2005). Large-scale pseudotachylytes and fluidized cataclasites from an ancient subduction thrust fault. *Geology*, *33*(12), 937. https://doi.org/10.1130/G21856.1

Ruthven, R., Singleton, J., Seymour, N., Gomila, R., Arancibia, G., Stockli, D. F., et al. (2020). The geometry, kinematics, and timing of deformation along the southern segment of the Paposo fault zone, Atacama fault system, northern Chile. *Journal of South American Earth Sciences*, *97*, 102355. https://doi.org/10.1016/j.jsames.2019.102355

Scheuber, E., & González, G. (1999). Tectonics of the Jurassic-Early Cretaceous magmatic arc of the north Chilean Coastal Cordillera (22°–26°S): A story of crustal deformation along a convergent plate boundary. *Tectonics*, *18*(5), 895–910. https://doi.org/10.1029/1999TC900024

Scheuber, E., Hammerschmidt, K., & Friedrichsen, H. (1995). $^{40}Ar/^{39}Ar$ and Rb-Sr analyses from ductile shear zones from the Atacama Fault Zone, northern Chile: The age of deformation. *Tectonophysics*, *250*(1–3), 61–87. https://doi.org/10.1016/0040-1951(95)00044-8

Seymour, N. M., Singleton, J. S., Mavor, S. P., Gomila, R., Stockli, D. F., Heuser, G., & Arancibia, G. (2020). The relationship between magmatism and deformation along the intra-arc strike-slip Atacama fault system, northern Chile. *Tectonics*, *39*(3), e2019TC005702. https://doi.org/10.1029/2019TC005702

Shishkina, T. A., Botcharnikov, R. E., Holtz, F., Almeev, R. R., & Portnyagin, M. V. (2010). Solubility of H_2O- and CO_2-bearing fluids in tholeiitic basalts at pressures up to 500 MPa. *Chemical Geology*, *277*(1–2), 115–125. https://doi.org/10.1016/j.chemgeo.2010.07.014

Sibson, R. H. (1973). Interactions between temperature and pore-fluid pressure during earthquake faulting and a mechanism for partial or total stress relief. *Nature Physical Science*, *243*(126), 66–68. https://doi.org/10.1038/physci243066a0

Sibson, R. H. (1975). Generation of pseudotachylyte by ancient seismic faulting. *Geophysical Journal of the Royal Astronomical Society*, *43*(3), 775–794. https://doi.org/10.1111/j.1365-246X.1975.tb06195.x

Sibson, R. H. (1981). Fluid flow accompanying faulting: Field evidence and models. In D. W. Simpson, & P. G. Richards (Eds.), Earthquake prediction: An International Review (Vol. 4, pp. 593–603). https://doi.org/10.1029/ME004p0593

Sibson, R. H., & Toy, V. G. (2006). The habitat of fault-generated pseudotachylyte: Presence vs. absence of friction-melt. In Geophysical Monograph Series (Vol. 170, pp. 153–166). https://doi.org/10.1029/170GM16

Spray, J. G. (1992). A physical basis for the frictional melting of some rock-forming minerals. *Tectonophysics*, *204*(3–4), 205–221. https://doi.org/10.1016/0040-1951(92)90308-S

Spray, J. G. (1995). Pseudotachylyte controversy: Fact or friction? *Geology*, *23*(12), 1119. https://doi.org/10.1130/0091-7613(1995)023<1119:PCFOF>2.3.CO;2

Ujiie, K., Tsutsumi, A., Fialko, Y., & Yamaguchi, H. (2009). Experimental investigation of frictional melting of argillite at high slip rates: Implications for seismic slip in subduction-accretion complexes. *Journal of Geophysical Research: Solid Earth*, *114*(4), 1–12. https://doi.org/10.1029/2008JB006165

Ujiie, K., Yamaguchi, H., Sakaguchi, A., & Toh, S. (2007). Pseudotachylytes in an ancient accretionary complex and implications for melt lubrication during subduction zone earthquakes. *Journal of Structural Geology*, *29*(4), 599–613. https://doi.org/10.1016/j.jsg.2006.10.012

Veloso, E. E., Gomila, R., Cembrano, J., González, R., Jensen, E., & Arancibia, G. (2015). Stress fields recorded on large-scale strike-slip fault systems: Effects on the tectonic evolution of crustal slivers during oblique subduction. *Tectonophysics*, *664*, 244–255. https://doi.org/10.1016/j.tecto.2015.09.022

Violay, M., Di Toro, G., Nielsen, S., Spagnuolo, E., & Burg, J. P. (2015). Thermo-mechanical pressurization of experimental faults in cohesive rocks during seismic slip. *Earth and Planetary Science Letters*, *429*, 1–10. https://doi.org/10.1016/j.epsl.2015.07.054

Violay, M., Nielsen, S., Gibert, B., Spagnuolo, E., Cavallo, A., Azais, P., et al. (2014). Effect of water on the frictional behavior of cohesive rocks during earthquakes. *Geology*, *42*(1), 27–30. https://doi.org/10.1130/G34916.1

Wallace, P. J., Kamenetsky, V. S., & Cervantes, P. (2015). Melt inclusion CO_2 contents, pressures of olivine crystallization, and the problem of shrinkage bubbles. *American Mineralogist*, *100*(4), 787–794. https://doi.org/10.2138/am-2015-5029

Williams, J. N., Toy, V. G., Smith, S. A. F., & Boulton, C. (2017). Fracturing, fluid-rock interaction and mineralisation during the seismic cycle along the Alpine Fault. *Journal of Structural Geology*, *103*, 151–166. https://doi.org/10.1016/j.jsg.2017.09.011